# Spaceborne Multiple-Swath SAR Imaging with Frequency Scanning

João Pedro Turchetti Ribeiro, Gerhard Krieger, Thomas Kraus, Markus Bachmann, and Alberto Moreira
Microwaves and Radar Institute, German Aerospace Center (DLR), 82234 Weßling, Germany

## Abstract

This paper presents innovative multiple-swath SAR imaging modes making use of the frequency scanning technique (F-Scan). A novel technique is proposed for high-resolution wide-swath imaging based on analogue beamforming, a less complex and inexpensive option compared to conventional digital beamforming systems. The separation of the swaths in both the time and frequency domains is considered. The performance is assessed for different scenarios, confirming the high performance and high flexibility that can be achieved with the proposed imaging modes. For instance, the possibility to image a contiguous 380 km swath with a resolution below 25 $m^2$ is shown.

## 1 Introduction

Synthetic aperture radar (SAR) is a remote sensing technique that enables a versatile imaging of Earth's surface. Its ability to obtain high-resolution images in any weather and independent of daylight makes it of special interest for monitoring the dynamic processes on Earth [1].

In order to achieve such a continuous monitoring with high-quality data, the development of SAR systems capable of acquiring wide swaths with high resolution is fundamental. For conventional single-channel systems, there is a clear trade-off between the scene size and the azimuth resolution, i.e., the improvement of one leads to the deterioration of the other. The task of achieving high-resolution wide-swath images, therefore, is not straightforward.

The first developments to overcome this limitation were explored by Currie and Brown in 1991 by taking advantage of the inherent versatility of phased-array antennas and the use of multiple channels [2]. For instance, they suggested the use of multiple elevation beams to cover different subswaths to increase the coverage. Similarly, in azimuth, the technique commonly known as the displaced phase centers antenna (DPCA) was also proposed. It consists of transmitting with a broad beam and receiving with many beams via multiple channels to improve the azimuth resolution.

Further developments of these techniques were brought by Suess et al. in 2001 [3, 4], who suggested the use of separate transmit and receive antennas allowing for the optimization of the RF design. The system proposed consists of a small broad-beam transmit antenna with high power and low losses by making use of traveling wave tubes, and a dedicated multi-channel antenna on receive applying what is today known as digital beamforming (DBF) both in azimuth and in elevation.

Later in 2008, Krieger et al. published a comprehensive investigation of high-resolution wide-swath imaging techniques with the use of a monostatic system [5], in which the wide transmit beams are obtained by amplitude and phase tapering. It was also proposed to use multiple waveforms together with dividing the transmit pulse into subpulses, which would be separated by means of DBF on receive. More interestingly for this research, the concept of intra-pulse beamsteering was introduced, i.e., transmitting first to far range and scanning towards near range. This approach leads to benefits in terms of shorter receive echo windows, wider swaths, and more homogeneous signal-to-noise ratio (SNR) performance across wide swaths.

A relatively simple implementation of such a continuous beamsteering was proposed by Roemer in 2017 [6, 7] through a technique known as frequency scanning (F-Scan). The idea behind F-Scan is to employ a pencil-beam antenna in elevation whose pointing varies as a function of the frequency. This scan from far to near range is achieved with the sole use of phase shifters and true time delay lines. Such an analog beamsteering, when compared to DBF implementations, has benefits in terms of lower hardware complexity and costs. Moreover, the use of a pencil-beam both on transmit and on receive leads to improvements in SNR. The drawback is the distribution of the total transmit bandwidth across the scene, thus reducing the range resolution.

The paper at hand refers to the development of multiple-swath imaging modes that take advantage of both the clever multi-channel strategies, and also of the more cost-effective analog beamsteering of F-Scan. First, the differentiation of the subswaths in the time domain by means of the concurrent technique with F-Scan is discussed. It consists of interleaving, from pulse to pulse, two independent modes, allowing for the generation of two images in a single flyover. Second, the innovative separation of the subswaths in the frequency domain is introduced. The idea is based on transmitting with F-Scan to a very wide swath, and receiving the echoes in multiple echo windows. The echoes are filtered in the space-frequency domain with the analogue beamsteering of F-Scan, and the blind ranges are filled with a two-burst ScanSAR approach. The concepts presented here are patent pending [8].

The paper is structured as follows. In section 2, the concurrent imaging of two swaths with independent modes is presented. Section 3 introduces a novel imaging technique which combines the multiple-elevation-beam ScanSAR with F-Scan. Finally, section 4 concludes the paper, summarizing the main outcomes and findings of this research, and also delineating the outlook for further work.

## 2 Concurrent Imaging with F-Scan

Concurrent imaging is the concept of simultaneously acquiring two or more scenes during the same flyover. Acquiring more than two scenes, although possible from a technical point of view, would lead to degradation of the imaging performance due to the sharing of the azimuth sampling, such that here only two scenes are considered. The feasibility of this concept was demonstrated in [9].

The concurrent technique consists of interleaving the transmission and reception of the two acquisition modes from pulse to pulse. For instance, one can interleave two stripmap (SM) acquisitions pointing towards different incidence angles (from here on called concurrent SM/SM imaging). The two swaths have flexibility to be distant up to a few hundred kilometers for the spaceborne application. The main benefit is not having to wait for the next satellite flyover to image the two areas of interest.

Such a concurrent imaging with F-Scan can then be implemented in three main manners: two stripmaps (SM/SM), two spotlights (ST/ST), or a mix of stripmap and spotlight (SM/ST). The azimuth pointing of the spotlight in this case would need to be preferably achieved with electronic beamsteering, requiring, therefore, enough antenna elements in azimuth to reduce the deterioration caused by grating lobes. The visualization of such imaging techniques are respectively depicted in **Figures 1a - 1c**. For the reduced swath widths of the spotlight acquisitions, the beam width may be already enough to cover the whole swath, making the use of F-Scan not necessary.

In the time domain, **Figure 2** depicts the signals involved in an exemplary concurrent SM/SM acquisition. The transmit signals using up and down chirp modulation are shown in blue and red, respectively. The arrival of the echoes and their respective frequency components are depicted in green and brown, while the nadir echoes are in orange and purple. This representation highlights the time-domain differentiation of the swaths.

The primary drawbacks of the concurrent imaging technique on a conventional SAR system like TerraSAR-X, as introduced in [9], are the limited scene sizes and the worse range ambiguity-to-signal ratios (RASR) achieved as a consequence of the need to double the pulse repetition frequency (PRF) because of the interleaving. As an attempt to tackle such degradation by reducing the PRF, concerns on the azimuth ambiguity-to-signal ratio (AASR) arise. F-Scan was investigated with the purpose of improving both the scene size and the range ambiguity performance of the concurrent imaging. First results showed that indeed the scene size can be increased by about 50 % with a system designed to use F-Scan [10]. A second-order benefit is the possibility to increase the maximum distance of the swaths due to the better RASR performance; a consequence of the use of pencil beams.

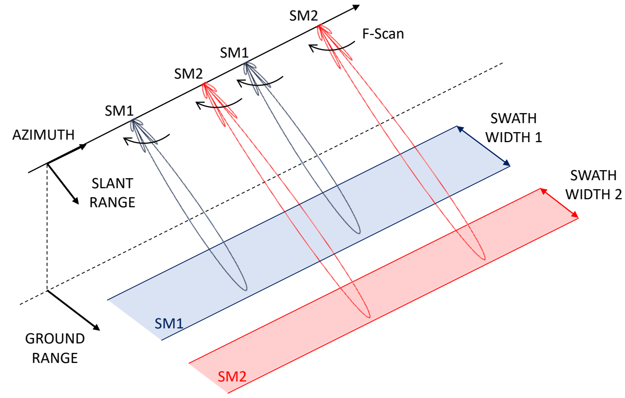


**(a)** Two stripmap images (SM/SM).

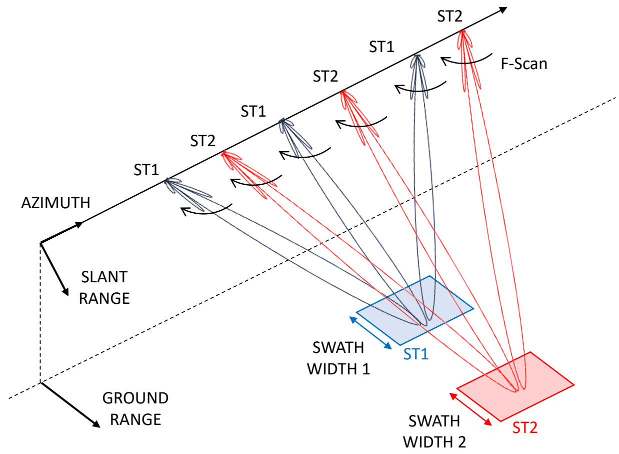


**(b)** Two spotlight images (ST/ST).

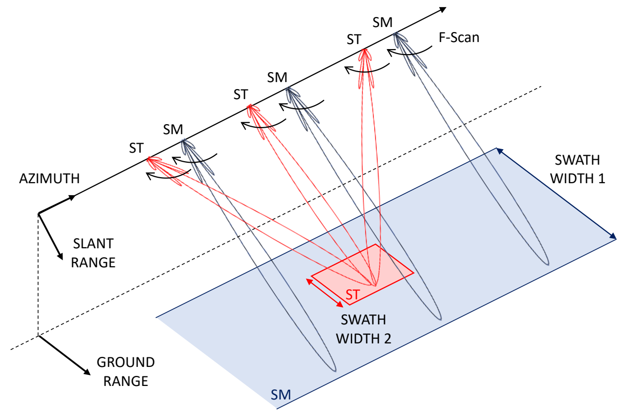


**(c)** One stripmap and one spotlight image (SM/ST). The scenes can also be disjoint.

**Figure 1** Schematic representations of the concurrent imaging with F-Scan.

The system parameters assumed in this work are based on the X-band HRWS mission proposal [11, 12]. Besides F-Scan, two important capabilities are expected, namely the availability of a bandwidth of 1200 MHz, and DPCA with four azimuth phase centers. These allow for higher resolution in range and azimuth, respectively. An additional requirement due to DPCA is a more strict PRF selection to obtain sampling close to uniformity. This PRF range is constrained based on the degradation of the SNR and of the

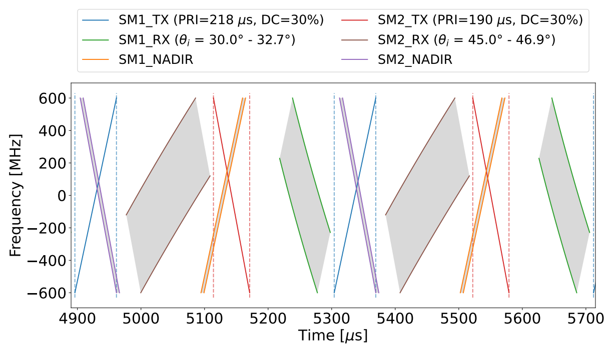


**Figure 2** Schematic time-frequency representation of the transmit and receive events of a concurrent SM/SM acquisition with F-Scan. Each subswath has a width of 30 km, and they are 190 km apart.

AASR. In range, the SNR degradation caused by the high bandwidth is compensated by the bigger antenna size.

A Monte Carlo simulation of concurrent SM/SM acquisitions around the globe resulted in the performance summarized in **Table 1**. The 2D resolution is given as the product of the ground range by the azimuth resolution after the antenna pattern and the Hamming window corrections. The ambiguity performance values represent the 95$^{th}$ percentile.

A total scene size of 50 km with a 1 m$^2$ resolution, combined with good ambiguity ratios and a high global availability highlights the excellent performance of such concurrent imaging technique with F-Scan. Additionally, the fact that the two 25 km swaths can be from 80 km up to 350 km apart brings a notable flexibility to the imaging of disjoint and far away targets. An in-depth analysis of this technique will be made available in [13].

The downside of such a technique is that it is tailored to image two relatively narrow swaths with high resolution, so that everything in between is not imaged. In the next section, a technique that fills this gap with more subswaths at the cost of a degraded spatial resolution will be described.

**Table 1** Summary of the performance of the concurrent SM/SM imaging mode achieved with F-Scan and DPCA.

| | **SM/SM with F-Scan** |
|---|---|
| **Antenna size** | 1.4 m (El.) / 6.0 m (Az.) |
| **Bandwidth** | 1200 MHz |
| **Swath width** | 2x 25 km |
| **Distance (swaths)** | 80 - 350 km |
| **Resolution ($\theta_i$ = 25°)** | 1.1 m$^2$ |
| **Resolution ($\theta_i$ = 45°)** | 0.48 m$^2$ |
| **RASR** | -29 dB |
| **AASR** | -21 dB |
| **Availability rate** | 95.4 % |

# 3 Multiple-Elevation-Beam ScanSAR with F-Scan

## 3.1 Imaging concept

Monostatic SAR systems aiming at obtaining very wide swaths typically would need to employ both a very low PRF and a very long antenna. Then, by using many receive channels in azimuth, the resolution could be improved to the desired levels. This solution, however, is not very adequate, as the antenna ends up being too long and the number of channels would be too high to obtain a high resolution. For instance, to image a 200 km swath, a PRF lower than 800 Hz and an antenna longer than 20 m would be required, leading to an unfeasible design.

A clever solution is to receive the echoes from the wide swath in multiple echo windows, maintaining the PRF relatively high and the antenna short. These overlapping echoes from the multiple subswaths are commonly seen as range ambiguities in conventional imaging. The use of DBF on receive (generation of multiple elevation beams) has been suggested in the literature to spatially filter the ambiguous echoes. This technique is, nevertheless, complex and hard to realize within restricted budgetary [11].

In this work, an innovative differentiation of these echoes – ambiguous in the time domain – is suggested. The employment of the analogue beamsteering of F-Scan is considered, allowing for the echoes to be distinguished in the space-frequency domain with a much simpler technique.

A consequence of receiving the echoes in multiple echo windows is that they are unavoidably interrupted by the transmit pulses. It causes the occurrence of blind ranges, i.e., because the radar cannot receive while it is transmitting, samples in range are missed. Several concepts to overcome such blind ranges were discussed in [14], namely the use of PRI variation and a variety of ScanSAR approaches.

The approach taken in this research for eliminating the gaps is the two-burst ScanSAR. It consists basically of performing two wide-swath bursts over the same region, but with slightly different PRFs. The PRFs are selected so that there is no overlap between the gaps of the bursts. By doing so, one burst covers the gaps of the other, leading to a final fully covered wide swath. Such imaging technique is visualized in **Figure 3**.

This approach for the elimination of the gaps is of relative simple implementation, and also favors the use of higher duty cycles. This characteristic is of great use for F-Scan, as it leads not only to a better SNR but also to a higher compression of the echoes on receive. Another feature of this technique is that those targets that are in neither of the gaps are imaged twice, giving the potential to improve the radiometric resolution and the SNR in these parts of the scene.

Concerning the ScanSAR aspects, the azimuth resolution is deteriorated by a factor of three when two bursts are considered. This loss can be recovered by the use of multiple azimuth phase centers. For instance, considering the mission proposal HRWS previously mentioned, a roughly

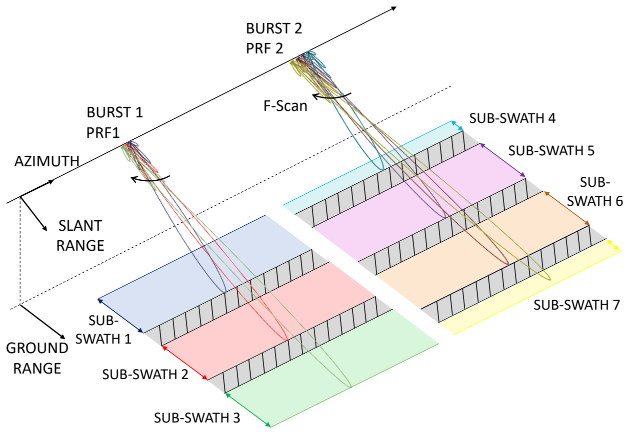


**Figure 3** Imaging concept of the two-burst multiple-elevation-beam ScanSAR with F-Scan. Different PRFs are used so that the gaps of the bursts do not overlap, leading to a final fully covered wide swath.

5 m azimuth resolution can be achieved with this two-burst mode. It represents an excellent performance improvement when compared to current deployed systems, which have an azimuth resolution of about 40 m to obtain such very wide swaths of up to 300 km, as many bursts are required, and only one channel is available in azimuth.

## 3.2 Performance

Due to the difference in slant range of the targets in the wide swath, the azimuth FM rate is significantly different for the near and the far ranges. Additionally, because all subswaths are imaged with the same burst duration, the azimuth resolution is range dependent.

An interesting opportunity arises with F-Scan to compensate for such dependency, as different center frequencies are transmitted towards each range position. An equalized azimuth resolution is obtained when the product $\lambda \cdot R$ is constant, i.e., when the Doppler shift is the same across the swath. For very wide swaths, the wavelength variation of the 1200 MHz bandwidth may not be enough to get the equalization, but at least some compensation is achieved by transmitting with lower frequencies towards the near range, and higher frequencies towards the far range. Considering the wavelength variation of F-Scan, the azimuth spectrum sharing of ScanSAR and the additional samples of DPCA, the azimuth resolution is finally given by

$$\delta_{\mathrm{az}} = \frac{0.886\,\gamma_{\mathrm{w,a}}}{2\,v_{\mathrm{s}}\,t_{\mathrm{b}}}\,\lambda\,R\,, \tag{1}$$

where $v_s$ is the satellite speed, $\gamma_{\mathrm{w,a}}$ the broadening factor of the Hamming window in azimuth, and $t_{\mathrm{b}}$ the burst duration.

A similar behavior is present in range, where the ground range resolution varies with the incidence angle. The varying wavelength of F-Scan causes also a varying half-power beamwidth (HPBW), leading to higher effective bandwidths for those targets imaged with lower frequencies. Here the condition for an equalized performance is the product $\lambda \cdot \sin\theta_{\mathrm{i}}$ being constant, with $\theta_{\mathrm{i}}$ being the incidence angle. Once again, using a down chirp for the far to near scanning helps to compensate also the ground range resolution variation. The ground range resolution considering such HPBW variation and also a linear frequency scanning is given by

$$\delta_{\mathrm{gr}} \approx \frac{c_0}{2\,B_{\mathrm{t}}}\,\frac{h\,\Delta\beta}{\lambda\,\sin\theta_{\mathrm{i}}}\,\gamma_{\mathrm{w,r}}, \tag{2}$$

where $c_0$ is the speed of light in free space, $B_{\mathrm{t}}$ the total transmit bandwidth, $h$ the antenna height, $\Delta\beta$ the total antenna scanning, and $\gamma_{\mathrm{w,r}}$ the broadening factor of the Hamming window in range.

The performance achieved with the imaging mode described here is summarized in **Table 2** for three scenarios. To exemplify the flattening of the resolution achieved when employing the higher frequencies at far range, **Figure 4** highlights the resolution curves as a function of the incidence angle for both up and down chirps for the scenario 1. The main benefits of such flattening are a more uniform performance across the scene, and also a better 2D resolution after multi-looking is applied to obtain square pixels.

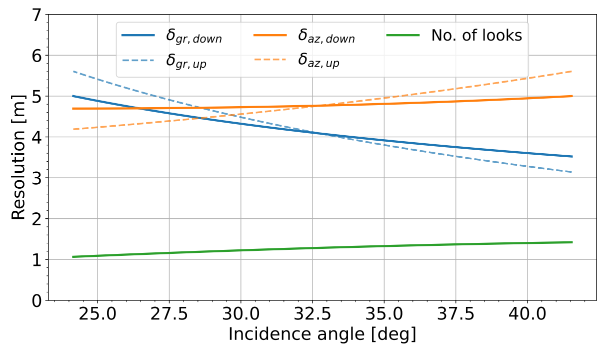


**Figure 4** Azimuth and ground range resolutions as a function of the incidence angle for the scenario 1 depicted in **Table 2**. The plot highlights the flattening of both resolution curves that can be achieved with down chirps. The plot also shows the number of looks at each incidence angle assuming a 2D resolution of 25 $m^2$.

In terms of the noise-equivalent sigma zero (NESZ), the use of a pencil beam both on transmit and on receive is a strong benefit of F-Scan in comparison to other schemes that transmit with a wide beam, such as SCORE. On the downside, a high total transmit bandwidth is required to achieve good range resolution for the individual targets, as the bandwidth is spread across the scene. One could argue that this lower effective bandwidth would improve the SNR, however, this benefit is equally lost by the lower effective illumination (or dwell) time of each target on ground.

The method considered to eliminate the gaps (two-burst ScanSAR) also benefits the SNR, as it allows for higher duty cycles; in this case 30 % is used based on [12].

A further contribution comes from the use of DPCA, which reduces the antenna gain on transmit and on receive. On transmit, typically a separate small antenna or only one element would be used to achieve the wide beam, thus also leading to a lower transmit power. However, as investigated in [15], a wide beam can also be achieved using

**Table 2** Summary of the performance of the multiple-elevation-beam ScanSAR imaging mode achieved with F-Scan and DPCA for a few exemplary scenarios.

| Scenario | Inc. angle | Swath width | Az. res. | Gr. res. | NESZ | AASR | RASR |
|---|---|---|---|---|---|---|---|
| 1 | 24°-41° | 200 km | 5 m | < 5 m | < -23.2 dB | < -26.3 dB | < -46.5 dB |
| 2 | 30°-52° | 300 km | 5 m | < 5 m | < -20.4 dB | < -24.4 dB | < -37.2 dB |
| 3 | 33°-57° | 380 km | 5 m | < 5 m | < -18.7 dB | < -22.9 dB | < -30.2 dB |

the whole antenna and applying only a quadratic phase tapering, consequently maintaining the total transmit power available from all the elements. On receive, the lower gain of each individual azimuth channel is equally compensated by the increase in the number of samples. Finally, disregarding the multi-channel reconstruction noise scaling, the NESZ is given by

$$\mathrm{NESZ} = \frac{16\pi\lambda}{P_{\mathrm{av}} l^2 h^2} \frac{k_{\mathrm{B}} T B_{\mathrm{t}} F L}{c_0 N_{\mathrm{DPCA}}} v_s R^3 \sin\theta_{\mathrm{i}} \cdot \frac{\int \frac{W^2(f)}{G^2_{\mathrm{el,norm}}(f,\beta)}\, df}{\int W^2(f)\, df} \frac{\int \frac{W^2(f_{\mathrm{d}})}{G^2_{\mathrm{az,norm}}(f_{\mathrm{d}})}\, df_{\mathrm{d}}}{\int W^2(f_{\mathrm{d}})\, df_{\mathrm{d}}}, \tag{3}$$

where $P_{\mathrm{av}} = 2.3\,\mathrm{kW}$ is the average transmit power, $l = 1.5\,\mathrm{m}$ the antenna size of each azimuth channel, $k_{\mathrm{B}}$ the Boltzmann constant, $T = 290\,\mathrm{K}$ the system noise temperature, $F = 3.7\,\mathrm{dB}$ the system noise figure, $L = 2\,\mathrm{dB}$ the system loss, $W(f)$ the Hamming window, $G_{\mathrm{el,norm}}(f,\beta)$ the normalized one-way antenna power pattern in elevation which depends both on the frequency and the pointing of interest (target position), and $G_{\mathrm{az,norm}}(f_{\mathrm{d}})$ the normalized antenna pattern in azimuth as a function of the Doppler frequency. The NESZ is computed for the scenarios 1 and 3 given in **Table 2**, and are depicted in **Figure 5**.

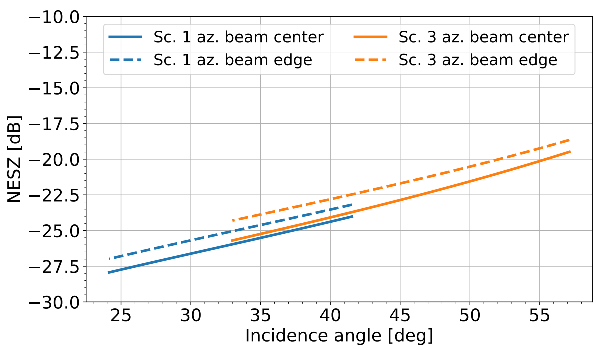


**Figure 5** NESZ obtained for the scenarios 1 and 3 depicted in **Table 2** according to (3). The ScanSAR scalloping effect is visible when comparing the NESZ of the targets at the center and at the edge of the azimuth beam.

Additional important performance parameters are the ambiguity-to-signal ratio in azimuth (AASR) and in range (RASR). As depicted in Table 2, the RASRs achieved are excellent. This is a consequence of employing pencil beams both on transmit and on receive, leading to a strong suppression of the ambiguous signals. In azimuth, on the other hand, the PRF does not need to be reduced to fit the wide swaths, as gaps are intentionally present in the imaging, thus guaranteeing sufficient suppression of the ambiguities. The noise scaling and reconstruction errors are not included in the results shown in Table 2, but are expected not to be an issue, as investigations show that PRFs close to the uniform-sampling case are sufficient to avoid the overlapping gaps.

## 3.3 Discussions

Conventional single-channel ScanSAR imaging is characterized by the use of several bursts to achieve wide swaths. As a consequence, the Doppler bandwidth and the resolution are typically very low. The Doppler spectrum, then, is highly sensitive to orbit and pointing deviations, leading to challenges in terms of a high spectral decorrelation. This aspect hinders the use of traditional ScanSAR to repeat-pass interferometric applications, as it would require a very tight orbit control and pointing accuracy. The ScanSAR mode described in this research is considerably less sensitive to such effects. First, the use of multiple azimuth channels broadens the beam and also the Doppler spectrum, making it less sensitive to the aforementioned errors. Additionally, because only two bursts are considered, the spectrum is not as strongly divided between the subswaths.
When compared to conventional imaging, one peculiar aspect of F-Scan is the fact that, for a fixed system, the range resolution deteriorates with increasing swath width due to the bandwidth spread. Therefore, in case the two-burst imaging mode described here is intended to obtain ultra-wide swaths (400 km or more), the range resolution would be highly deteriorated. In complete divergence with traditional ScanSAR, the final image would have reasonably good azimuth resolution, but an impaired range resolution. In order to obtain a more balanced performance, the range resolution can be recovered by reducing the swath width of each burst, and increasing the number of bursts at different incidence angles. For instance, one could think of a ScanSAR imaging comprised of a first burst with a relatively short swath and no blind ranges at a lower incidence angle to compensate the range-to-ground projection with the higher effective bandwidth, and then two more bursts, as here described, with gaps and wider swath at a higher incidence angle. Preliminary investigations show the potential to obtain 500 km scenes with 50 $\mathrm{m}^2$ resolution with such a method.
A further optimization can be achieved by implementing

subpulses for each subswath, a technique previously introduced by Bordoni et al. in [16, 17]. The motivation arises from the fact that it is not necessary to transmit to the blind ranges, i.e., some frequencies may not need to be transmitted, as they will not be received. The benefits of this technique would be a higher dwell time for the targets effectively imaged – meaning a better overall SNR –, and also the potential to tailor the performance of each subswath by adjusting the FM rate of each subpulse.

# 4 Conclusion

The imaging modes described in this paper demonstrate the potential of multiple-swath imaging with F-Scan, mainly in terms of high performance and high flexibility. First, the concurrent technique with F-Scan was shown to achieve high resolution and great ambiguity levels, with the swaths being up to hundreds of kilometers apart. Second, the innovative idea of imaging several subswaths, and to use F-Scan to filter the signals in the space-frequency domain was introduced. Such a technique is of great value, as it can increase the capabilities of the already proposed mission HRWS without adding new system requirements. It was shown that the two-burst ScanSAR with F-Scan manages to increase the total swath width up to 380 km with a 2D resolution of 5 x 5 $m^2$. It is important to highlight that a strong advantage of this mode is that no DBF in elevation is required, meaning the system complexity is drastically lower in comparison with techniques such as SCORE.

As an outlook for further work, other techniques to cover the blind ranges, such as staggered SAR [18] and slow PRI variation [19] can be investigated. These would eliminate the need of ScanSAR, thus significantly improving the azimuth resolution. Other challenges would arise, such as the required high azimuth oversampling factor and the onboard processing. The subpulses technique and the use of more bursts are also envisaged for future investigations.

# 5 Literature


[1] A. Moreira, P. Prats-Iraola, M. Younis, G. Krieger, I. Hajnsek, and K. P. Papathanassiou, "A tutorial on synthetic aperture radar," *IEEE Geoscience and Remote Sensing Magazine*, vol. 1, no. 1, pp. 6–43, 2013.

[2] A. Currie and M. Brown, "Wide-swath SAR," *IEE Proceedings F Radar and Signal Processing*, vol. 139, no. 2, pp. 122–135, 1992.

[3] M. Suess, B. Grafmueller, and R. Zahn, "A novel high resolution, wide swath SAR system," in *Proc. IEEE Geosci. Remote Sens. Symp. (IGARSS)*. Sydney, NSW, Australia: IEEE, 2001.

[4] M. Suess and W. Werner Wiesback, "Side-looking synthetic aperture radar system," European Patent Applicant: EADS Astrium GmbH. EP 1 241 487 B1, 2002, publication Date: 18 Sept. 2002.

[5] G. Krieger, N. Gebert, and A. Moreira, "Multidimensional waveform encoding: A new digital beamforming technique for synthetic aperture radar remote sensing," *IEEE Transactions on Geoscience and Remote Sensing*, vol. 46, pp. 31–46, 2008.

[6] C. Roemer, "Introduction to a new wide area SAR mode using the F-Scan principle," in *Proc. IEEE Geosci. Remote Sens. Symp. (IGARSS)*, Fort Worth, USA, 2017, pp. 3844–3847.

[7] ——, "High resolution wide swath synthetic aperture system," International Patent WO 2019/015 911 A1, 2019.

[8] J. P. T. Ribeiro, T. Kraus, M. Bachmann, A. Moreira, and G. Krieger, "Synthetik-apertur-radarverfahren," German Patent 10 2023 113 029.3, 2023.

[9] T. Kraus, J. P. T. Ribeiro, M. Bachmann, U. Steinbrecher, and C. Grigorov, "Concurrent imaging for TerraSAR-X: Wide-area imaging paired with high-resolution capabilities," *IEEE Transactions on Geoscience and Remote Sensing*, vol. 60, pp. 1–14, 2022.

[10] J. P. T. Ribeiro, T. Kraus, M. Bachmann, and R. Machado, "Introducing F-Scan to the concurrent imaging mode," in *Proc. International Radar Symposium (IRS)*, Berlin, Germany, 2023, pp. 1–10.

[11] A. Moreira, M. Zink, M. Bartusch, A. E. N. Quiroz, and S. Stettner, "German spaceborne SAR missions," in *Proc. 2021 IEEE Radar Conference*, Atlanta, USA, 2021, pp. 1–6.

[12] J. Mittermayer, G. Krieger, A. Bojarski, M. Zonno, M. Villano, M. Pinheiro, M. Bachmann, S. Buckreuss, and A. Moreira, "MirrorSAR: An HRWS add-on for single-pass multi-baseline SAR interferometry," *IEEE Transactions on Geoscience and Remote Sensing*, vol. 60, pp. 1–18, 2022.

[13] J. P. T. Ribeiro, T. Kraus, M. Bachmann, R. Machado, G. Krieger, and A. Moreira, "Concurrent SAR imaging with F-Scan: Timing design and performance prediction," *IEEE Transactions on Geoscience and Remote Sensing*, 2023, submitted.

[14] G. Krieger, N. Gebert, M. Younis, F. Bordoni, A. Patyuchenko, and A. Moreira, "Advanced concepts for ultra-wide-swath SAR imaging," in *Proc. EUSAR*. Friedrichshafen, Germany: VDE, 2008.

[15] M. Villano, G. Krieger, and A. Moreira, "Advanced spaceborne SAR systems with planar antenna," in *Proc. IEEE Radar Conference*. Seattle, WA, USA: IEEE, 2017.

[16] F. Bordoni, M. Younis, and G. Krieger, "Performance investigation on the high-resolution wide-swath SAR system operating in multisubpulse mode," in *Proc. IEEE Geosci. Remote Sens. Symp. (IGARSS)*. Munich, Germany: IEEE, 2012, pp. 3568–3571.

[17] F. Bordoni, G. Krieger, and M. Younis, "Multifrequency subpulse SAR: Exploiting chirp bandwidth for an increased coverage," *IEEE Geoscience and Remote Sensing Letters*, vol. 16, pp. 40–44, 2019.

[18] M. Villano, G. Krieger, and A. Moreira, "Staggered SAR: High-resolution wide-swath imaging by continuous PRI variation," *IEEE Transactions on Geoscience and Remote Sensing*, vol. 52, no. 7, 2014.

[19] F. Q. de Almeida, M. Younis, P. Prats-Iraola, M. Rodriguez-Cassola, G. Krieger, and A. Moreira, "Slow pulse repetition interval variation for high-resolution wide-swath SAR imaging," *IEEE Transactions on Geoscience and Remote Sensing*, vol. 59, pp. 5665–5686, 2021.